Open Journal of Geology, 2023, 13, 487-503
https://www.scirp.org/journal/ojg
ISSN Online: 2161-7589
ISSN Print: 2161-7570

Temporal Variability of Extreme Precipitation in Jiangxi during 1961-2018

Kaimei Zhang[1], Fengen Huang[1*], Zijie Huang[2], Hua Yang[1]

[1]Meteorological Service Center of Jiangxi Province, Jiangxi Meteorological Bureau, Nanchang, China
[2]Meteorological Bureau of Yihuang County, Fuzhou, China
Email: 350035113@qq.com, *466808961@qq.com, 31749395@qq.com, 19558512@qq.com

How to cite this paper: Zhang, K.M., Huang, F.G., Huang, Z.J. and Yang, H. (2023) Temporal Variability of Extreme Precipitation in Jiangxi during 1961-2018. *Open Journal of Geology*, **13**, 487-503.
https://doi.org/10.4236/ojg.2023.135022

Received: February 13, 2023
Accepted: May 28, 2023
Published: May 31, 2023

Abstract

Using 58 years (1961 to 2018) of daily rainfall data, this study focuses on determining trends in the annual and seasonal precipitation extremes of Jiangxi, China, by choosing four extreme precipitation indices, including strong precipitation amount (SPA), mean precipitation intensity (MPI), strong precipitation days (SPD), and strong precipitation frequency (SPF). The monotonic trends are tested by using the Mann-Kendall test for the trends and Sen's method for the magnitude of the trends. The effective sample size (ESS) method was used to eliminate the influence of serial correlation in the Mann-Kendall test. The results indicated that station Zixi had the strongest extreme precipitation, while Wanzai had the weakest. The trends for each index showed an obvious regional feature over Jiangxi. Increasing trends in annual extreme precipitation indices were found at almost all stations, and the annual variability of the extreme precipitation indices was pronounced, especially for the mean precipitation intensity and the strong precipitation frequency; the majority of these positive trends were shown by the statistical tests. In spring, four indices exhibited significant increasing trends in Northeast and Southwest Jiangxi; however, in summer, only MPI had a remarkable positive trend across almost all of Jiangxi. For the other indices, few stations had remarkable trends. In autumn, MPI and SPF showed remarkable increasing trends in most regions of Jiangxi, while SPA and SPD showed increasing trends at only 6 stations and 3 stations, respectively, which were scattered in the northern and middle parts. In winter, the stations with remarkable upward trends in SPA and SPD were mainly located in the middle of the region, whereas the significant patterns of MPI and SPF were located in the south and middle of the region.

Keywords

China, Precipitation Amount, Mean Precipitation Intensity, Strong Precipitation Days

1. Introduction

In recent decades, global climate change has captured a large amount of attention by worldwide scholars [1] [2] [3] [4] [5] owing to its devastating effects on human life, the environment, and social and ecological implications [6]. In addition to changes in global climate, atmospheric circulation anomalies [7] [8], surface evaporation [9], and so on, these factors all influence precipitation extremes. From a global perspective, Frich *et al.* [10] found a significant increase in extreme precipitation events, although spatial variation patterns show strong regional characteristics. Otherwise, trends in extreme precipitation have been largely studied on specific regional and national scales around the world [11]-[16]. The majority of regions that have been exposed to extreme precipitation events, such as in America [17] [18] [19] [20], Europe [13] [14] [21] [22], and Asia [23] [24], are displaying an increasing trend. However, no significant trends were detected in Africa [25].

Previous studies have shown that the trends of extreme precipitation events around the world have regional and seasonal diversity. On a national scale, a small trend has been shown for total precipitation amount [26] [27]; however, on the whole, the amount, frequency and intensity of extreme precipitation in China exhibit an upward trend [28] while showing regional characteristics [29] [30].

Regionally, increasing trends in precipitation extremes have been found in Northwest China [4] [31], Southwest China [24] [32], East China [33] [34] and South China [27], although decreasing trends have been observed in North China [35] [36] [37] and Northeast China [38].

Any positive or increasing trend in extreme precipitation is a serious concern [39]. However, compared to more developed cities, Jiangxi, a large agricultural province that is extremely vulnerable to flood and landslide hazards [40] [41] [42], has not received enough concern, and no comprehensive studies have been carried out in relation to climate change. This study focuses on detecting the trends of four annual and seasonal extreme precipitation indices as well as the magnitude of the trends in Jiangxi using the Mann-Kendall test and Sen's slope estimator. The effective sample size (ESS) method, defined as a modified Mann-Kendall test in this title, was employed to eliminate the influence of serial correlation. Although this is not the first study employing Mann-Kendall test and Sen's slope estimator for precipitation over China [43], it is the first analysis of precipitation extremes over china using the ESS method.

2. Materials and Methods

2.1. Study Area Description

Jiangxi (**Figure 1**) is situated at approximately 24˚29'N to 30˚04'N latitude and 113˚34'E to 118˚28'E longitude, encompassing a total area of approximately 105,000 km^2. Jiangxi is a southern province in the People's Republic of China, spanning from the banks of the Yangtze River in the north to the hillier areas of

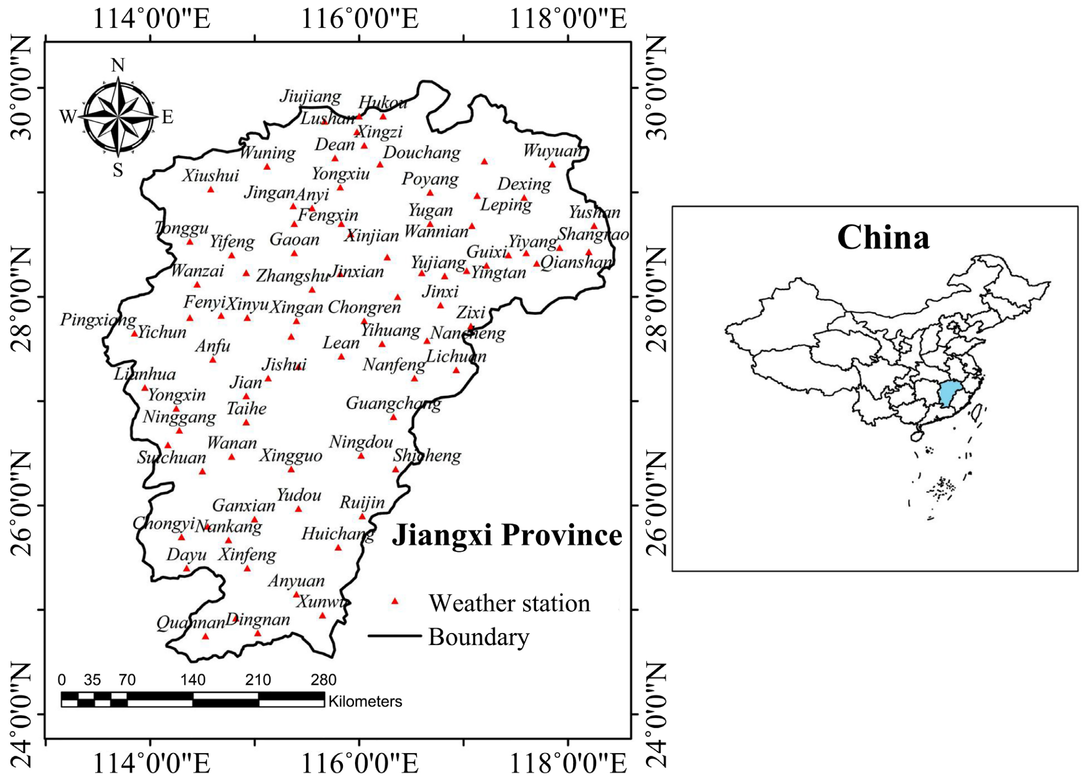

Figure 1. Locations of meteorological stations in Jiangxi province.

the south. Mountains surround Jiangxi on three sides, with the Mufu Mountains, Jiuling Mountains, and Luoxiao Mountains to the west, the Huaiyu Mountains and Wuyi Mountains to the east, and the Jiulian Mountains and Dayu Mountains to the south. In addition, the Gan River dominates the province, flowing through its entire length from south to north. It enters Lake Poyang in the north, which is the largest freshwater lake in China. The region has a subtropical monsoon climate, with the mean annual precipitation from 1424 mm to 1995 mm. The annual precipitation is largely concentrated in the rainy season from March to September and decreases from northwest to southeast (**Figure 2(a)**). Above all, Jiangxi was selected as the study area due to its unique geographical location.

2.2. Data and Data Pre-Processing

In this study, the daily precipitation records from 50 representative meteorological stations were obtained from Jiangxi Provincial Meteorological Information Center. The locations of the weather stations in Jiangxi can be found in **Figure 1**. Jiangxi has more than 90 synoptic stations. However, only 50 stations have consistent quality records. The 58-year period between1961 and 2018 was considered as the study duration to ensure an adequate record length. The daily data were used to calculate the seasonal and annual precipitation, which were used in the trend analysis. Definitions of extreme precipitation thresholds are various. Some studies choose a fixed precipitation value as a threshold and determine that precipitation greater than this threshold is extreme precipitation. For example,

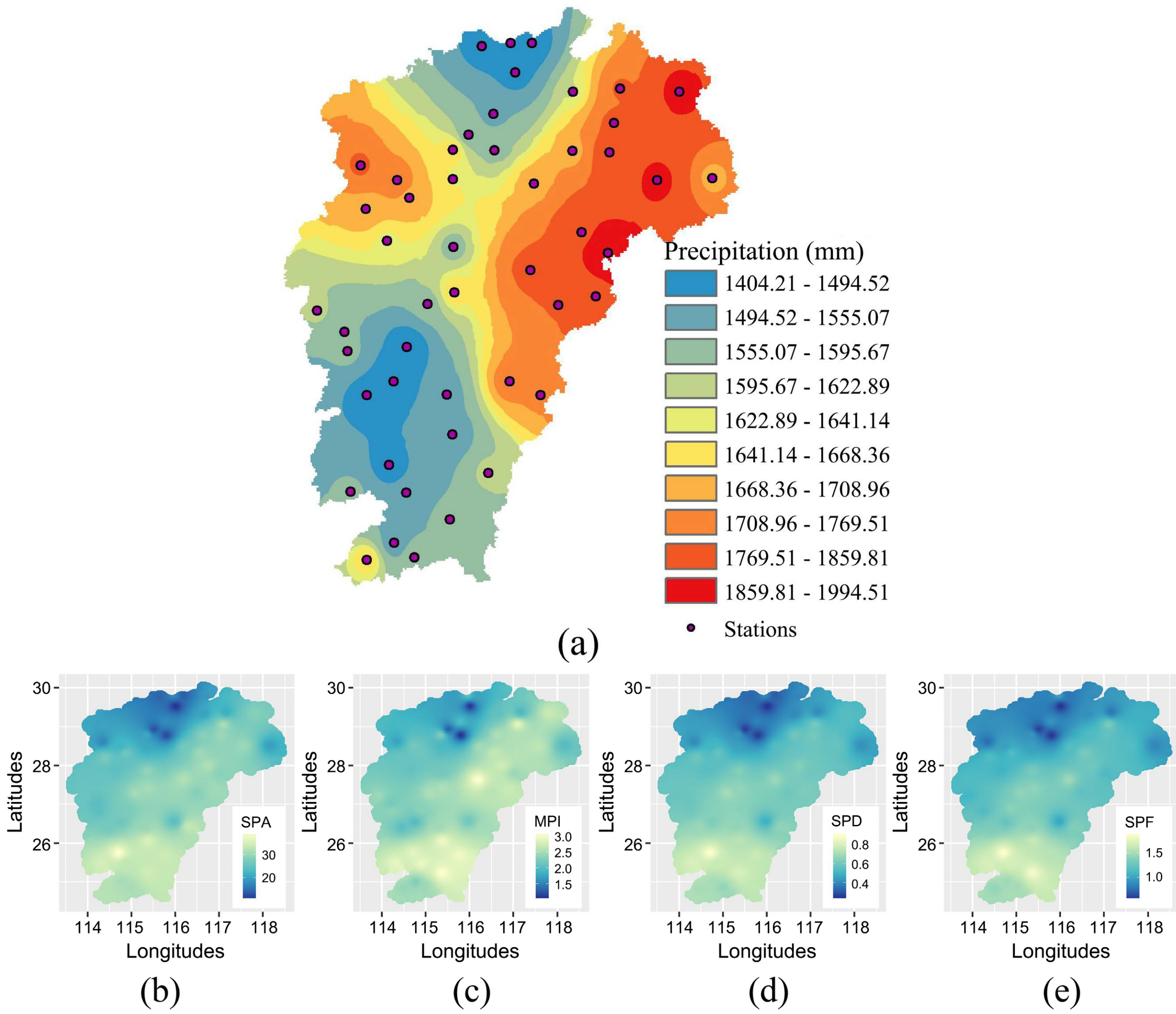

Figure 2. Spatial distribution of rainfall amount and four extreme precipitation indices in Jiangxi during 1961-2018: (a) total rainfall amount, (b) SPA, (c) MPI, (d) SPD, (e) SPF.

China generally refers to precipitation events with daily precipitation over 50 mm as heavy rains and daily precipitation over 25 mm is called heavy rain. In fact, Different regions have individual climates and natural environments; thus, if only absolute thresholds are used to define daily precipitation extremes, there would be a lack of comparability between the various regions. Currently, a percentile value is used to denote the threshold and has been widely employed to research extreme weather events caused by global climate change [10] [44] [45]. In this paper, using daily precipitation data from Jiangxi, the thresholds of extreme were estimated in terms of the 95th percentiles, and the precipitation extremes were identified. Four indices of extreme precipitation (strong precipitation amount (SPA), mean precipitation intensity (MPI), strong precipitation day (SPD) and strong precipitation frequency (SPF)) were used to describe flood hazards. A detailed definition of each index is described in **Table 1**.

Table 1. Statistical indices of strong precipitation and their definition.

Term	Definition	Unit
Strong precipitation amount (SPA)	Total precipitation amount for top 5% of all wet events	mm
Mean precipitation intensity (MPI)	The average daily precipitation amount (conditional)	mm/day
Strong precipitation days (SPD)	The total days for daily precipitation amount for top 5% of all wet events	day
Strong precipitation frequency (SPF)	The percentage of SPA days from rain days (conditional)	%

2.3. Methodology

The modified Mann-Kendall test, Sen's slope estimator and ArcGIS software were employed for the trend analyses. The modified Mann-Kendall test and Sen's slope estimator were used for detecting and estimating trends in the time series of the annual and seasonal values of strong precipitation indices. For monotonic trend analysis, the non-parametric Mann-Kendall test was used, and for slope of linear trend estimation, the non-parametric Sen's slope estimator was used. There are three phases in trend analysis. First, the modified Mann-Kendall test was used to identify the tendency of strong precipitation indices at 4 significance levels, including 0.1 (+), 0.05 (*), 0.01 (**) and 0.001 (***). Second, Sen's method was employed to calculate the magnitude of the trend, and finally, ArcGIS 9.3 was applied to map the spatial distribution of stations with significant changes in tendency at the different significance levels.

2.3.1. Modifying the Mann-Kendall Test

The non-parametric Mann-Kendall test, used to detect a statistically significant trend in a time series, has been widely used to examine randomness and trends in hydrology and climatology [11] [36]. The Mann-Kendall statistic S of the precipitation series x is calculated by the formula:

$$s = \sum_{i=1}^{n-1} \sum_{j=i+1}^{n} \operatorname{sgn}\left(x_j - x_i\right), \tag{1}$$

Here, sgn is the signum function. The variance associated with S is computed by the following equation:

$$\operatorname{Var}(S) = \frac{n(n-1)(2n+5) - \sum_{i=1}^{m} t_i (t_i - 1)(2t_i + 5)}{18}, \tag{2}$$

Here, m is the number of tied groups and t_i is the number of data points in the i^{th} group. In cases where the sample size n > 10, the test statistic Z was calculated using the formula:

$$Z = \begin{cases} \dfrac{S-1}{\sqrt{\operatorname{Var}(S)}} & \text{if} \quad S > 0 \\ 0 & \text{if} \quad S = 0, \\ \dfrac{S+1}{\sqrt{\operatorname{Var}(S)}} & \text{if} \quad S < 0 \end{cases} \tag{3}$$

Positive (negative) values of Z denote increasing (decreasing) trends. When examining either upward or downward monotonic trends at each significance level, the null hypothesis of no trend was rejected for an absolute value of Z greater than $Z1 - a/2$, as obtained from the standard normal cumulative distribution tables [44].

Missing values are allowed, and the data need not be distributed normally. The Mann-Kendall test has some of the same priorities; however, positive serial correlation will increase the possibility of rejecting the null hypothesis of no trend, which is actually true; in contrast, negative correlation will reduce the possibility of rejecting the null hypothesis of no trend [45]. Durbin and Watson indicated that the rainfall data exhibited serial correlation [46]. Thus, the ESS method [47] was applied to correct the influence of serial correlation by modifying the variance of the Mann-Kendall statistic. The modified variance of S is given by Equation (4):

$$\mathrm{Var}^{*}(S) = \mathrm{Var}(S) \cdot \frac{n}{n^{*}}, \tag{4}$$

Here, n^* is the ESS. The formula provided by Matalas and Langbein was used to calculate n* for the lag-1 autoregressive process [47]:

$$n^{*} = \frac{n}{1 + 2 \cdot \dfrac{\rho_1^{n+1} - n \cdot \rho_1^2 + (n-1)\rho_1}{n(\rho_1 - 1)^2}}, \tag{5}$$

Here, n^* is lag-1 serial correlation, by replacing the variance Var(s) with $\mathrm{Var}^*(s)$, the original Mann-Kendall statistic, Z is replaced by Z^* in Equation (6). According to this test, the modified Mann-Kendall statistic was used to identify any significant tendency of the strong precipitation indices.

$$Z^{*} = Z\sqrt{\frac{n^{*}}{n}}, \tag{6}$$

2.3.2. Sen's Slope Estimator

If a time series is assumed to have a linear trend, then the true slope of the existing trend **Figure 2(a)** shows the distribution of rainfall amount over Jiangxi from 1961 to 2018. The geographical distribution of precipitation is generally increasing from west to east. **Figures 2(b)-(e)** gives the distribution of four indices of extreme precipitation. As shown, however, the distribution of SPA was similar to SPD while MPI was similar to SPF, the four indices had some similar spatial features. Wuyi Mountain area over the eastern part of central Jiangxi showed a large value area for all the indices, moreover, Poyang Lake sediments alluvial plain area and western part of central Jiangxi showed a low value area, and the spatial distribution of total precipitation also had the two similar features. However, we calculated the correlation coefficients between site elevation and extreme precipitation, total precipitation respectively. The results showed a significant positive correlation between four extreme precipitation indices and the topography, which all passed the significance level test of $a = 0.01$, while the correlation between total precipitation and topography sex was not significant.

Extreme precipitation in the high altitude area is stronger and more easily lead to water erosion, debris flow and other issues (as change per unit time) can be estimated by using a consistent non-parametric procedure [25]; Sen's slope estimator, combined with the M-K test, is often used to reveal the trend and amplitude of variation and is defined by

$$f(t) = Qt + B, \tag{7}$$

$$Q_i = \frac{x_i - x_j}{j - i}, \tag{8}$$

Here, Q is the slope of trend, B is a constant and t is time. Q_i is Sen's slope estimator of the slope, and x_i and x_j are numerical data at times i and j ($j > i$), respectively, if the series length of values is N, the overall slope is defined by Equation (9).

$$Q = \begin{cases} Q_{\text{med}} = Q_{\frac{N+1}{2}} & N \text{ is odd} \\ Q_{\text{med}} = \frac{1}{2}\left(Q_{\frac{N}{2}} + Q_{\frac{N+2}{2}}\right) & N \text{ is even} \end{cases}, \tag{9}$$

Finally, a two-sided normal distribution test for is given at the 100 (1 − *a*) % confidence level, and the true slope may be obtained by a non-parametric test. In this study, the magnitudes of strong precipitation indices were examined by using the procedure in MAKESENS, which was developed by Salmi *et al.* [48].

3. Results and Analyses

3.1. Spatial Variation of Annual Precipitation

Figure 2(a) shows the distribution of rainfall amount over Jiangxi from 1961 to 2018. The geographical distribution of precipitation is generally increasing from west to east. **Figures 2(b)-(e)** gives the distribution of four indices of extreme precipitation. As shown, however, the distribution of SPA was similar to SPD while MPI was similar to SPF, the four indices had some similar spatial features. Wuyi Mountain area over the eastern part of central Jiangxi showed a large value area for all the indices, moreover, Poyang Lake sediments alluvial plain area and western part of central Jiangxi showed a low value area, and the spatial distribution of total precipitation also had the two similar features. However, we calculated the correlation coefficients between site elevation and extreme precipitation, total precipitation respectively. The results showed a significant positive correlation between four extreme precipitation indices and the topography, which all passed the significance level test of *a* = 0.01, while the correlation between total precipitation and topography sex was not significant. Extreme precipitation in the high altitude area is stronger and more easily lead to water erosion, debris flow and other issue.

3.2. Annual Trends

Annual mean, annual trends and the amplitudes (in mm/year) of four extreme precipitation indices are given in Table 2. As shown, the annual trends found by the modified Mann-Kendall test were almost similar to the trends exposed by Sen's slope estimator. In addition to the SPA of one station (Poyang) and the SPDs of three stations (Shanggao, Dayu, Xinfeng) that showed negative trends, the other extreme precipitation indices series had positive trends. Station Zixi, with an SPA of 272 mm, an MPI of 5.7 mm/day, an SPD of 15.6 day and an SPF of 7.2, showed the strongest extreme precipitation, while Wanzai showed the weakest extreme precipitation.

Table 2. Mean annual, values of statistics Z^* of the modified Mann-Kendall test and Q of the Sen's slope estimator for extreme precipitation indices.

Station	SPA			MPI			SPD			SPF		
	Mean Annual	Z^*	Q	Mean Annual	Z^*	Q	Mean Annual	Z^*	Q	Mean Annual	Z^*	Q
Tonggu	694.9	0.84	2.5	8.7	3.02 **	0.056	12.4	0.59	0	5.6	2.11 *	0.043
Yifeng	725.8	0.82	1.824	8.5	2.25 *	0.03	12.1	0.94	0.029	6	1.58	0.026
Wanzai	271.8	0.80	1.438	5.7	2.94 **	0.033	5.2	0.61	0	2.7	1.55	0.021
Shanggao	465.2	0.04	0.07	6.5	3.53 ***	0.047	8	−0.13	0	3.7	1.63	0.025
lianhua	438.1	0.49	1.019	6.6	3.30 ***	0.041	7.9	1.37	0.03	3.5	2.68 **	0.039
Fenyi	467.7	1.73 +	2.95	6.6	3.71 ***	0.043	8.2	1.15	0.036	3.8	2.44 *	0.044
Xiaping	578.3	2.33 *	5.216	7.4	3.66 ***	0.071	9.5	2.69 **	0.095	4.7	3.23 **	0.076
Yongxin	492.2	1.40	2.686	6.9	3.31 ***	0.043	8.3	1.75 +	0.067	3.9	2.56 *	0.055
Wanan	677.6	1.67 +	3.15	8.1	2.45 *	0.027	10.3	1.43	0.047	5	2.10 *	0.035
Suichuan	753	1.31	2.192	8.1	2.05 *	0.017	12.7	1.51	0.045	5.1	2.01 *	0.032
Taihe	367.9	2.04 *	3.414	6	2.61 **	0.032	6.4	1.94 +	0.071	3.3	2.49 *	0.053
Nankang	515.7	0.54	0.942	7.1	3.04 **	0.027	9.4	0.27	0	4.1	1.17	0.018
Dayu	812.3	0.39	0.33	8.7	2.92 **	0.025	13.2	−0.46	0	5.5	0.61	0.007
Xinfeng	511.1	0.67	0.853	7.3	3.33 ***	0.032	8.9	−0.11	0	4.3	1.72 +	0.02
Jiujiang	779.6	0.12	0.095	8.8	2.11 *	0.032	13.8	0.66	0	5.6	1.62	0.027
Ruichang	516.7	1.44	2.684	7.5	2.72 **	0.044	8.8	1.98 *	0.056	4	2.68 **	0.05
Yongxiu	579.5	1.01	2.767	7.8	2.41 *	0.038	10	0.99	0.036	4.7	1.65 +	0.033
Hukou	365.4	0.58	1.184	6.3	1.78 +	0.029	6.7	0.76	0.024	3.4	1.26	0.031
Xinzi	392.3	0.67	1.668	6.8	1.50	0.02	7.1	1.11	0.026	3.6	1.27	0.022
Poyang	594.5	−0.05	−0.065	8.5	1.56	0.022	10.6	0.41	0	5.1	1.07	0.02
Jing dezhen	572.1	1.30	4.231	8.1	3.30 ***	0.083	10.7	0.88	0.03	5.1	2.23 *	0.052
Wuyuan	497.1	1.33	4.132	7.8	3.25 **	0.074	8.6	1.23	0.038	4.1	2.53 *	0.05
fengxin	849.1	1.30	3.013	9.6	2.93 **	0.038	13.9	0.92	0.026	6.9	1.65 +	0.029
Anyi	634.4	0.60	0.967	8.1	2.52 *	0.04	11	0.64	0	5.4	1.62	0.027
Gaoan	456.8	1.35	2.84	6.8	3.13 **	0.05	8	1.42	0.04	3.7	2.23 *	0.04
Yugan	458.8	1.70	3.916	7.3	3.27 **	0.073	8.2	1.58	0.063	4.6	2.75 **	0.065

Continued

Jinxian	443.3	3.23	7.465	7.6	3.46 ***	0.053	8.2	3.52	0.122	3.9	3.82 ***	0.077
Wannian	523.2	0.80	2.177	8.1	2.65 **	0.05	9.5	1.34	0.042	5.1	2.27 *	0.045
Dongxiang	611.4	1.81 +	4.385	8.1	3.38 ***	0.067	10.6	1.64	0.059	5.2	2.61 **	0.052
Leping	593.2	1.91 +	5.306	8	3.30 ***	0.079	10.8	1.69 +	0.07	5.1	2.61 **	0.067
Hengfeng	369.7	1.89 +	6.138	7	2.43 *	0.043	6.7	1.93 +	0.1	3.4	2.14 *	0.058
Guangfeng	646.7	1.55	3.721	9.1	1.53	0.025	12.2	1.59	0.056	6.3	1.84 +	0.033
Xinjian	646.6	1.50	3.367	8.5	2.13 *	0.036	11	1.59	0.042	5.2	1.90 +	0.036
Xingan	734.5	1.55	4.111	8.6	2.97 **	0.057	12.1	2.18 *	0.075	5.6	3.14 **	0.068
Yongfeng	744.5	1.37	2.843	9.8	3.17 **	0.064	11.9	2.26 *	0.069	6.5	3.42 ***	0.067
Jishui	555.2	1.35	2.22	7.9	3.25 **	0.039	9.5	2.06 *	0.061	5	3.06 **	0.048
Jinxi	786.2	1.74	4.227	8.9	2.44 *	0.033	13.7	2.29 *	0.083	6	2.68 **	0.059
Zixi	970.4	2.00	5.269	10.7	3.76 ***	0.083	15.6	2.57 *	0.091	8	3.65 ***	0.079
Yihuang	864.9	1.84 +	3.351	9.7	3.96 ***	0.089	13.8	2.09 *	0.073	7.2	2.98 **	0.082
Nanfeng	591.8	0.96	2.317	7.8	3.23 **	0.056	10.8	1.24	0.036	5.1	2.69 **	0.042
Lichuan	537.8	1.35	2.983	8.2	3.84 ***	0.074	9.8	1.98	0.056	5.1	3.51 **	0.057
Xingguo	804.8	2.03 *	3.785	9.8	2.67 **	0.03	13.9	1.05	0.029	6.7	1.94 +	0.034
Ningdu	479.5	1.56	3.38	8.3	2.97 **	0.036	7.9	1.33	0.042	4.8	2.11 *	0.035
Shicheng	530.7	1.43	3.025	8.6	1.46	0.019	9.2	1.09	0.03	5.6	1.55	0.023
Yudu	669.1	1.21	1.4	8.9	2.45 *	0.029	11.2	0.82	0	5.9	2.13 *	0.031
Huichang	701.4	1.38	1.943	9.3	3.90 ***	0.038	11.7	1.41	0.026	6.5	2.85 **	0.035
Anyuan	387.2	0.67	0.822	7.7	3.78 ***	0.043	7.1	0.93	0	4.2	2.87 **	0.045
Quannan	602.2	0.10	0.364	9.1	3.22 **	0.048	10.7	0.11	0	6.3	1.94 +	0.035
Longnan	474.1	1.46	2.61	8	3.28 **	0.045	8	1.71	0.048	4.7	2.92 **	0.043
Dingnan	916.9	0.45	0.79	10.8	3.50 ***	0.04	14.9	0.73	0	7.8	2.36 *	0.03

Note: ***, **, * and + indicate the trends are significant at 99.9%, 99%, 95% and 90% level of confidence, respectively.

Except for the SPA of Poyang, which had an insignificant negative trend of 0.05, the other stations showed positive trends, with series from nine stations showing a remarkable trend at the significance level. The significant increasing trends varied between 2.92 mm/year at Fenyi station and 6.14 mm/year at Hengfeng station. The significant increasing annual trends varied between 2.92 mm/year at Fenyi station and 6.14 mm/year at Hengfeng station.

All the trends of MPI were increasing. Moreover, significant increasing trends were found at almost all the stations, with thirty-five stations showing remarkable trends above the 95% confidence levels, which accounted for 70% of the stations. The significant positive annual trends of MPI ranged from 0.025 (Dayu station) to 0.089 mm/day (Yihuang station).

Similar to MPI, the mean annual SPF of all the stations, ranging from 2.7 percent for station Wanzai to 8 percent for station Zixi, was also increasing. Significant trends were detected at thirty-nine stations, accounting for 80% of the stations. Moreover, eighteen stations showed significant trends above the 95% confidence levels. The significant positive annual trends of SPF ranged from 0.025 (Dayu station) to 0.089 percent/day (Yihuang station).

In addition to three stations (Shanggao, Dayu and Xinfeng) with insignificant decreasing trends, the SPD of all the others were increasing. However, only twelve stations showed significant trends above the 90% confidence levels, which accounted for 24% of the stations. The significant positive annual trends of SPD ranged from 0.056 mm/year at Ruichang station to 0.1mm/year at Hengfeng station.

Above all, the increasing trends in extreme precipitation indices in Jiangxi were obvious, especially for MPI and SPF, and the majority of these positive trends were identified by the statistical tests.

Figure 3 presents the spatial distribution of stations with a remarkable trend in annual extreme precipitation indices at four significance levels (α = 0.001***, 0.01**, 0.05*, 0.1+). When comparing the stations distributions that had a remarkable trend of the four extreme precipitation indices, it shows that MPI and SPF have similar spatial distributions, and SPA is similar to SPD. The MPI of 46 stations and the SPF of 39 stations displayed significant upward trends at the $\alpha \leq 0.6$ significance level and were rather evenly distributed in the whole region. The SPA and SPF showed an increasing trend for 9 stations and 12 stations, respectively, which were mainly distributed in the northeast and central regions of Jiangxi.

3.3. Seasonal Trends

The modified Mall-Kendall test was also applied to detect the seasonal trends inprecipitation extremes for Jiangxi. Figures 4-7 shows a significant spatial distribution of extreme precipitation indices in four seasons: spring, summer, autumn and winter, respectively.

In spring, the significant spatial distributions of SPA and SPF were similar; the SPA of 14 stations and the SPF of 21 stations, mainly in the northeast and southwest of Jiangxi, demonstrated a remarkable trend at the $\alpha \leq 0.1$ significance

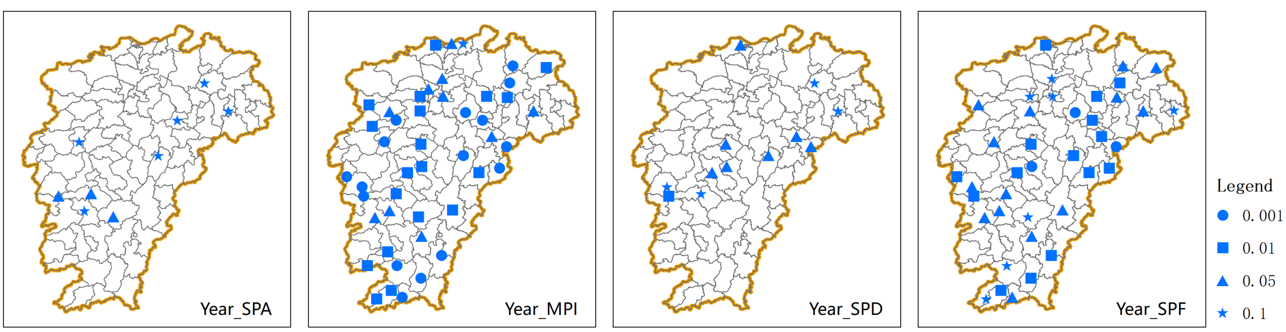

Figure 3. Spatial distribution of stations with a significant trend of annual extreme precipitation indices at the four significance levels.

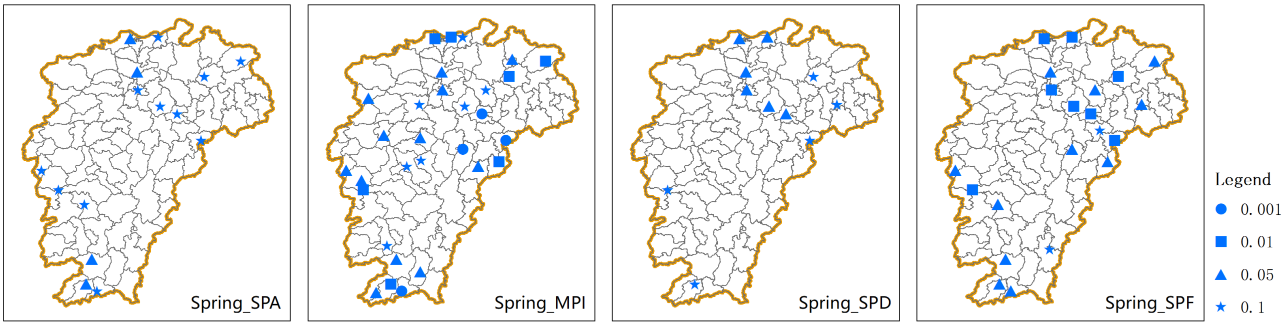

Figure 4. Spatial distribution of stations with a significant trend of extreme precipitation indices in spring at the four significance levels.

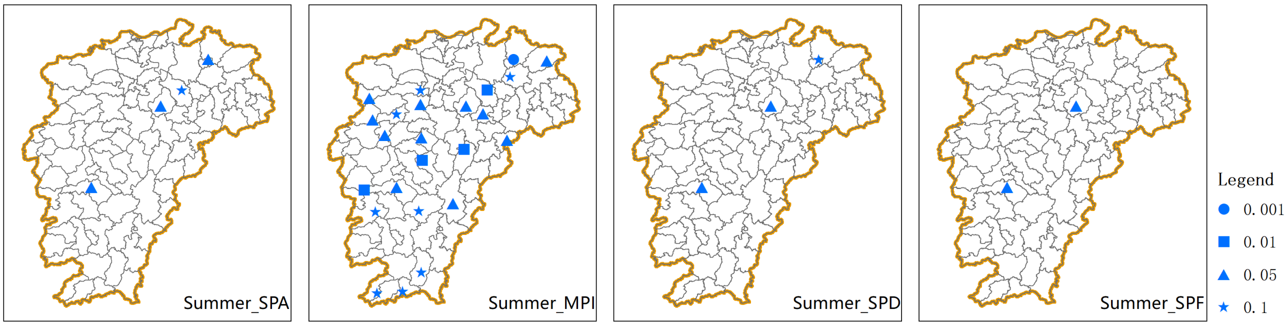

Figure 5. Spatial distribution of stations with a significant trend of extreme precipitation indices in summer at the four significance levels.

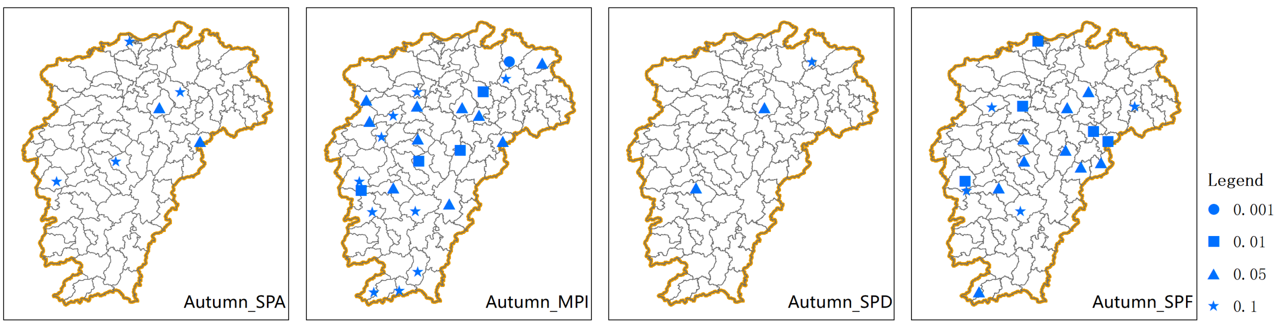

Figure 6. Spatial distribution of stations with a significant trend of extreme precipitation indices in autumn at the four significance levels.

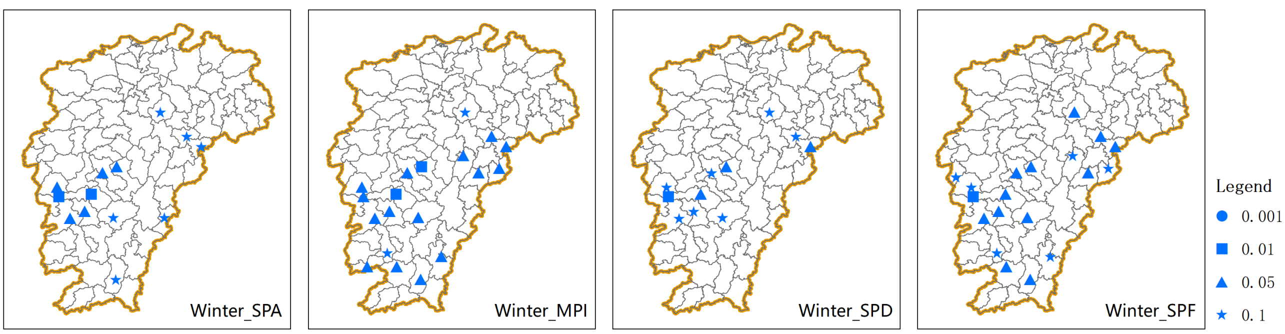

Figure 7. Spatial distribution of stations with a significant trend of extreme precipitation indices in winter at the four significance levels.

level. The MPI of 30 stations had significant trends. For SPD, 11 stations, mainly in the northeast, exhibited a remarkable increasing trend. The area northeast of Jiangxi exhibited a remarkable increasing trend for each index selected in the study.

In summer, SPA, SPD, and SPF exhibited significant upward trends for only 2 - 4 stations, including Taihe and Jinxian stations; the rest had no significant trends. However, the MPI of 24 stations showed a remarkable increasing trend, and the spatial distribution was similar to the pattern observed in the spring.

In autumn, the MPI of 25 stations and the SPF of 18 stations demonstrated significant positive trends ($\alpha \leq 0.6$), evenly distributed in Jiangxi, except for the northern region of South Jiangxi. The SPA and SPD showed an increasing trend for only 6 and 3 stations, respectively, which were scattered in the northern and middle regions.

In winter, the SPA, MPI, SPD and SPF had significant trends ($\alpha \leq 0.6$) for 13, 18, 11 and 19 stations, respectively. The SPA and SPD showed similar significant patterns, and the stations with remarkable upward trends were mainly located in the middle of the region, whereas the significant patterns of MPI and SPF were located in the southern and the middle of the region.

In general, the trend of seasonal precipitation extremes showed a diverse pattern. Under the background of a little change of total precipitation, precipitation events had an obvious trend of extremeness, and then the distribution of precipitation would have an obvious trend of extremeness, and the distribution of precipitation will become more asymmetric, which might bring with negative effects on the eco-environment, and especially the agricultural production in Jiangxi.

4. Results and Discussions

This study applied the M-K test, the Sen's estimator and GIS tools to recognize the trends and spatial variation of four extreme precipitation indices at 50 stations in Jiangxi between1961 and 2018. The results revealed a significant increasing trend in annual precipitation events for most parts of Jiangxi. In addition to the SPA of one station and the SPD of three stations that showed a negative trend, the rest had positive trends. Station Zixi showed the strongest extreme precipitation, with an SPA of 272 mm, an MPI of 5.7 mm/day, an SPD of 15.6 day and an SPF of 7.2, while Wanzai station showed the weakest extreme precipitation.

The trends of each index showed an obvious regional feature over Jiangxi, and the variability of the annual and seasonal precipitation extremes was most pronounced in Jiangxi. In spring, four indices showed remarkable increasing trends in Northeast and Southwest Jiangxi; however, in summer, only the MPI had a significant increasing trend across almost all of Jiangxi. For the other indices (SPA, SPD, SPF), few stations showed a remarkable trend. In autumn, the MPI and SPF showed remarkable increasing trends in most regions of Jiangxi, except for the northern part of southern Jiangxi; in contrast, the SPA and SPD showed an increasing trend for only 6 and 3 stations, respectively, scattered in the northern and middle parts. It can be deduced that moderate-intensity rainfall could be increasing more remarkably than extreme rainfall in summer and autumn, which caused mean precipitation intensity (MPI) in summer and autumn to show a significant increasing trend in most regions. In winter, for SPA and SPD, the stations with remarkable upward trends were mainly located in the middle of the region, whereas the significant patterns of MPI and SPF were located in the southern and middle parts of the region. It is concluded that winter extreme rainfall in the middle of Jiangxi had a significant increasing trend, while moderate-intensity rainfall was possibly more remarkable in the southern region of Jiangxi.

This study presents the analyses results for four extreme precipitation indices trends during the 58-year-period of 1961 to 2018. In conclusion, spring precipitation extremes in most regions of Jiangxi and winter extreme rainfall in the middle of Jiangxi showed significant increasing trends. In addition, winter moderate-intensity rainfall in the area south of Jiangxi had a more remarkable upward trend than precipitation extremes in general. However, in summer and autumn, for most regions in Jiangxi, moderate-intensity rainfall could be increasing more remarkably than extreme rainfall. Further studies are required to seek the causes and influencing factors affecting the spatial variation in trends of precipitation extremes. Moreover, rainfall amount trends (figures omitted) of only four stations demonstrated a remarkable trend at the $\alpha = 0.1$ significance level while most of stations showed that extreme precipitation indices series have had significant positive trends at the $\alpha \leq 0.1$ significance level. Under the background of a little change of total precipitation, precipitation events had an obvious trend of extremeness, and the distribution of precipitation, precipitation events had an obvious trend of extremeness, and the distribution of precipitation became more asymmetric, which might be one of the main causes of the higher frequency and enhanced intensity of drought and flood, and bring with negative effects on the eco-environment, and especially the agricultural production over Jiangxi. However, the forcing mechanisms of increasing precipitation extremes are very complicated and need to be studied in subsequent work.

Funding

Key research and development project of Jiangxi Province: Research on risk forecast and early warning technology of Jiangxi Expressway (20202BBGL73100);

Key Projects of Jiangxi Meteorological Bureau: The mining of meteorological tourism resources and research on characteristic landscape forecast technology in Jiangxi Province;

Key Projects of Jiangxi Meteorological Bureau: Research on Meteorological Forecast and Early Warning Technology for Ensuring Water Traffic Safety.

Conflicts of Interest

The authors declare no conflicts of interest regarding the publication of this paper.

References

[1] Agterberg, F. (2022) How Can Earth Science Help Reduce the Adverse Effects of Climate Change? *Journal of Earth Science*, **33**, 1338. https://doi.org/10.1007/s12583-022-1741-y

[2] Olsson, J. and Foster, K. (2013) Short-Term Precipitation Extremes in Regional Climate Simulations for Sweden. *Hydrology Research*, **45**, 479-489 https://doi.org/10.2166/nh.2013.206

[3] Onyutha, C., Nyekoogiramoi, P. and Willems, P. (2014) Uncertainties in Impact Assessment of Climate Change on Rainfall Extremes in the Lake Victoria Basin. 3*rd International Conference on Earth Science & Climate Change*, San Francisco, 28-30 July 2014, 28-30.

[4] Yin, J.B., Guo, S.L., Wang, J., *et al.* (2022) Thermodynamic Driving Mechanisms for the Formation of Global Precipitation Extremes and Ecohydrological Effects. *Science China Earth Sciences*, **66**, 92-110. https://doi.org/10.1007/s11430-022-9987-0

[5] Mtewele, Z.F., Xu, X.Y. and Jia, G.S. (2021) Heterogeneous Trends of Precipitation Extremes in Recent Two Decades over East Africa. *Journal of Meteorological Research*, **35**, 1057-1073. https://doi.org/10.1007/s13351-021-1028-8

[6] Oluwatimilehin, I.A., Akerele, J.O., Oladeji, T.A., Omogbehin, M.H. and Atai, G. (2022) Assessment of the Impact of Climate Change on the Occurrences of Malaria, Pneumonia, Meningitis, and Cholera in Lokoja City, Nigeria. *Regional Sustainability*, **3**, 309-318. https://doi.org/10.1016/j.regsus.2022.11.007

[7] Jiang, T., Zhang, Q., Zhu, D. and Wu, Y.J. (2006) Yangtze Floods and Droughts (China) and Teleconnections with ENSO Activities (1470-2003). *Quaternary International*, **14**, 29-37. https://doi.org/10.1016/j.quaint.2005.05.010

[8] Gong, D.Y., Yang, J., Kim, S.J., *et al.* (2011) Spring Arctic Oscillation-East Asian Summer Monsoon Connection through Circulation Changes over the Western North Pacific. *Climate Dynamics*, **37**, 2199-2216. https://doi.org/10.1007/s00382-011-1041-1

[9] Trenberth, K.E. (1998) Atmospheric Moisture Residence Times and Cycling: Implications for Rainfall Rates and Climate Change. *Climatic Change*, **39**, 667-694. https://doi.org/10.1023/A:1005319109110

[10] Frich, P., Alexander, L.V., Della-Marta, P., Gleason, B., Haylock, M., Tank, A.M.G.K. and Peterson, T. (2002) Observed Coherent Changes in Climatic Extremes during the Second Half of the Twentieth Century. *Climate Research*, **19**, 193-212. https://doi.org/10.3354/cr019193

[11] Alexander, L.V., Uotila, P. and Nicholls, N. (2009) Influence of Sea Surface Temperature Variability on Global Temperature and Precipitation Extremes. *Journal of Geophysical Research*: *Atmospheres*, **114**, D18116. https://doi.org/10.1029/2009JD012301

[12] Boberg, F., Berg, P., Thejll, P., Gutowski, W.J. and Christensen, J.H. (2010) Improved Confidence in Climate Change Projections of Precipitation Further Evaluated Using Daily Statistics from ENSEMBLES Models. *Climate Dynamics*, **35**, 1509-1520. https://doi.org/10.1007/s00382-009-0683-8

[13] Christensen, J.H. and Christensen, O.B. (2003) Climate Modelling: Severe Summertime Flooding in Europe. *Nature*, **421**, 805-806. https://doi.org/10.1038/421805a

[14] Fowler, H.J., Ekström, M., Blenkinsop, S. and Smith, A.P. (2007) Estimating Change in Extreme European Precipitation Using a Multimodel Ensemble. *Journal of Geo-

physical Research: *Atmospheres*, **112**, D18104. https://doi.org/10.1029/2007JD008619

[15] He, Y., Ye, J. and Yang, X. (2015) Analysis of the Spatio-Temporal Patterns of Dry and Wet Conditions in the Huai River Basin Using the Standardized Precipitation Index. *Atmospheric Research*, **166**, 120-128. https://doi.org/10.1016/j.atmosres.2015.06.022

[16] Tao, D., Tang, X., Li, X. and Wu, X. (2006) Asymmetric Bagging and Random Subspace for Support Vector Machines-Based Relevance Feedback in Image Retrieval. *IEEE Transactions on Pattern Analysis and Machine Intelligence*, **28**, 1088-1099. https://doi.org/10.1109/TPAMI.2006.134

[17] Donat, M.G. *et al*. (2013) Updated Analyses of Temperature and Precipitation Extreme Indices since the Beginning of the Twentieth Century: The HadEX2 Dataset. *Journal of Geophysical Research*: *Atmospheres*, **118**, 2098-2118. https://doi.org/10.1002/jgrd.50150

[18] Pryor, S.C., Howe, J.A. and Kunkel, K.E. (2009) How Spatially Coherent and Statistically Robust Are Temporal Changes in Extreme Precipitation in the Contiguous USA? *International Journal of Climatology*, **29**, 31-45. https://doi.org/10.1002/joc.1696

[19] de los Milagros Skansi, M., *et al*. (2013) Warming and Wetting Signals Emerging from Analysis of Changes in Climate Extreme Indices over South America. *Global and Planetary Change*, **100**, 295-307. https://doi.org/10.1016/j.gloplacha.2012.11.004

[20] Villarini, G. and Vecchi, G.A. (2012) Twenty-First-Century Projections of North Atlantic Tropical Storms from CMIP5 Models. *Nature Climate Change*, **2**, 604-607. https://doi.org/10.1038/nclimate1530

[21] Liu, Q., Yang, Z. and Cui, B. (2008) Spatial and Temporal Variability of Annual Precipitation during 1961-2006 in Yellow River Basin, China. *Journal of Hydrology*, **361**, 330-338. https://doi.org/10.1016/j.jhydrol.2008.08.002

[22] Pavan, V., Tomozeiu, R., Cacciamani, C. and Di Lorenzo, M. (2008) Daily Precipitation Observations over Emilia-Romagna: Mean Values and Extremes. *International Journal of Climatology*, **28**, 2065-2079. https://doi.org/10.1002/joc.1694

[23] Goswami, B.N., Venugopal, V., Sengupta, D., Madhusoodanan, M.S. and Xavier, P.K. (2006) Increasing Trend of Extreme Rain Events over India in a Warming Environment. *Science*, **314**, 1442-1445. https://doi.org/10.1126/science.1132027

[24] Wang, Y. and Zhou, L. (2005) Observed Trends in Extreme Precipitation Events in China during 1961-2001 and the Associated Changes in Large-Scale Circulation. *Geophysical Research Letters*, **32**, L09707. https://doi.org/10.1029/2005GL022574

[25] Sen Roy, S. and Rouault, M. (2013) Spatial Patterns of Seasonal Scale Trends in Extreme Hourly Precipitation in South Africa. *Applied Geography*, **39**, 151-157. https://doi.org/10.1016/j.apgeog.2012.11.022

[26] Wang, F., Yang, S., Higgins, W., Li, Q. and Zuo, Z. (2014) Long-Term Changes in Total and Extreme Precipitation over China and the United States and Their Links to Oceanic—Atmospheric Features. *International Journal of Climatology*, **34**, 286-302. https://doi.org/10.1002/joc.3685

[27] Zhai, P., Sun, A., Ren, F., Liu, X., Gao, B. and Zhang, Q. (1999) Changes of Climate Extremes in China. *Climatic Change*, **42**, 203-218. https://doi.org/10.1023/A:1005428602279

[28] Gao, T. and Xie, L. (2014) Study on Progress of the Trends and Physical Causes of

Extreme Precipitation in China during the Last 50 Years. *Advances in Earth Science*, **29**, 577-589.

[29] Min, S. and Qian, Y.F. (2008) Regionality and Persistence of Extreme Precipitation Events in China. *Advances in Water Science*, **19**, 763-771. (In Chinese)

[30] Wang, Z.F. and Qian, Y.F. (2009) Frequency and Intensity of Extreme Precipitation Events in China. *Advances in Water Science*, **20**, 1-9. (In Chinese)

[31] Jiang, F.Q., Hu, R.J., Wang, S.P., Zhang, Y.W. and Tong, L. (2013) Trends of Precipitation Extremes during 1960-2008 in Xinjiang, the Northwest China. *Theoretical and Applied Climatology*, **111**, 133-148. https://doi.org/10.1007/s00704-012-0657-3

[32] Li, Y.G., He, D., Hu, J.M. and Cao, J. (2015) Variability of Extreme Precipitation over Yunnan Province, China 1960-2012. *International Journal of Climatology*, **35**, 245-258. https://doi.org/10.1002/joc.3977

[33] Ding, Y., Wang, Z. and Sun, Y. (2008) Inter-Decadal Variation of the Summer Precipitation in East China and Its Association with Decreasing Asian Summer Monsoon. Part I: Observed Evidences. *International Journal of Climatology*, **28**, 1139-1161. https://doi.org/10.1002/joc.1615

[34] Wang, X.L. and Zhai, P.M. (2008) Changes in China's Precipitation for Various Categories during 1957-2004. *Journal of Tropical Meteorology*, **24**, 459-466.

[35] Alexander, L.V. *et al.* (2006) Global Observed Changes in Daily Climate Extremes of Temperature and Precipitation. *Journal of Geophysical Research*: *Atmospheres*, **111**, D05109.

[36] Fan, L., Lu, C., Yang, B. and Chen, Z. (2012) Long-Term Trends of Precipitation in the North China Plain. *Journal of Geographical Sciences*, **22**, 989-1001. https://doi.org/10.1007/s11442-012-0978-2

[37] Wang, J., Jiang, D.K. and Zhang, Y.J. (2012) Analysis on Spatial and Temporal Variation of Extreme Climate Events in North China. *Chinese Journal of Agrometeorology*, **33**, 166-173.

[38] Wang, B. *et al.* (2013) Changes in Extreme Precipitation over Northeast China, 1960-2011. *Quaternary International*, **298**, 177-186. https://doi.org/10.1016/j.quaint.2013.01.025

[39] Yin, Y., Chen, H., Xu, C.Y., Xu, W., Chen, C. and Sun, S. (2016) Spatio-Temporal Characteristics of the Extreme Precipitation by L-Moment-Based Index-Flood Method in the Yangtze River Delta Region, China. *Theoretical and Applied Climatology*, **124**, 1005-1022. https://doi.org/10.1007/s00704-015-1478-y

[40] Hong, H., Pourghasemi, H.R. and Pourtaghi, Z.S. (2016) Landslide Susceptibility Assessment in Lianhua County (China): A Comparison between a Random Forest Data Mining Technique and Bivariate and Multivariate Statistical Models. *Geomorphology*, **259**, 105-118. https://doi.org/10.1016/j.geomorph.2016.02.012

[41] Hong, H., Pradhan, B., Jebur, M.N., Bui, D.T., Xu, C. and Akgun, A. (2016b) Spatial Prediction of Landslide Hazard at the Luxi Area (China) Using Support Vector Machines. *Environmental Earth Sciences*, **75**, Article No. 40. https://doi.org/10.1007/s12665-015-4866-9

[42] Hong, H., Pradhan, B., Xu, C. and Bui, D.T. (2015) Spatial Prediction of Landslide Hazard at the Yihuang Area (China) Using Two-Class Kernel Logistic Regression, Alternating Decision Tree and Support Vector Machines. *Catena*, **133**, 266-281. https://doi.org/10.1016/j.catena.2015.05.019

[43] Fan, X.H. and Wang, M.B. (2010) Change Trends of Air Temperature and Precipitation over Shanxi Province, China. *Advances in Earth Science*, **29**, 577-589.

[44] Yue, S. and Wang, C.Y. (2004) The Mann-Kendall Test Modified by Effective Sample Size to Detect Trend in Serially Correlated Hydrological Series. *Water Resources Management*, **18**, 201-218. https://doi.org/10.1023/B:WARM.0000043140.61082.60

[45] Durbin, J. and Watson, G.S. (1951) Corrections to Part I: Testing for Serial Correlation in Least Squares Regression: I. *Biometrika*, **38**, 177-178. https://doi.org/10.2307/2332326

[46] Lettenmaier, D.P. (1976) Detection of Trends in Water Quality Data from Records with Dependent Observations. *Water Resources Research*, **12**, 1037-1046. https://doi.org/10.1029/WR012i005p01037

[47] Matalas, N.C. and Langbein, W.B. (1962) Information Content of the Mean. *Journal of Geophysical Research*, **67**, 3441-3448. https://doi.org/10.1029/JZ067i009p03441

[48] Salmi, T., Maatta, A., Anttila, P., Ruoho-Airola, T. and Amnell, T. (2002) Detecting Trends of Annual Values of Atmospheric Pollutants by the Mann-Kendall Test and Sen's Solpe Estimates—The Excel Template Application MAKESENS. Finish Meteorological Institute, Helsinki, 35 p.